Brandon, M.T., 2004, The Cascadia subduction wedge: the role of accretion, uplift, and erosion. in In: "Earth Structure, An Introduction to Structural Geology and Tectonics", by B.A. van der Pluijm and S. Marshak, Second Edition, WCB/McGraw Hill Press, p. 566-574

22.2 THE CASCADIA SUBDUCTION WEDGE: THE ROLE OF ACCRETION, UPLIFT, AND EROSION—An essay by Mark T. Brandon[1]

22.2.1 Introduction

Given the constant surface area of Earth, there must be a balance between the amount of plate created at spreading centers and the amount consumed at subduction zones and other sites of plate convergence. Today, 80% of this return flow occurs at subduction zones, and the other 20% at continent-continent collision zones and diffuse oceanic convergent zones. Modern subduction zones have a total length of 51,000 km, and consume plates at an average rate of 62 km/my (or 62 mm/y), with the highest rates (210 km/my, or 210 mm/y) being found along the Tonga Trench in the southwest Pacific. Subduction zones are marked by Benioff-zone earthquakes and active-arc volcanism, which are indications of shearing and bending of the cold subducting plate and melting caused by dehydration of the plate. Seismologists have generated tomographic images that show subducting plates penetrating deep into the interior of Earth, locally reaching the core-mantle boundary (see Chapter 14).

Subduction zones are not totally efficient in removing the subducting plate. Some fraction of the plate gets left behind as **accretionary complexes** that accumulate at the leading edge of the overriding plate (Figure 22.2.1). In some cases, this accretion might be episodic, involving the collision of large lithospheric blocks, called **tectonostratigraphic terranes.** More commonly, only the sedimentary cover of the downgoing plate is accreted, while the underlying crust and mantle lithosphere are fully subducted. The thickness of this sedimentary cover varies considerably, from hundreds of meters at oceanic subduction zones, like the Mariana system, to as much as 7 km at ocean-continent subduction zones, such as the Makran margin of southwest Pakistan. There is evidence from modern subduction zones that not all of the incoming sedimentary section is accreted. The global rate of sediment subduction has been estimated in one study to be equivalent to an average thickness of 300–500 m of compacted sedimentary rock along all subduction zones combined. This analysis, however, is complicated by deeply subducted sediment that may be accreted at depth beneath the overriding plate, rather than fully subducted into the mantle.

22.2.2 Accretionary Flux

An important theme of this essay is that accretion of largely sedimentary materials has a strong influence on deformation of the overriding plate at subduction zones. We are concerned here with the **accretionary flux** into the subduction zone, which is defined as the thickness of accreted materials times the rate of plate subduction. Sedimentary rocks are quickly compacted during the subduction process, so we use the equivalent thickness of fully compacted sedimentary rock when calculating the accretionary flux. This correction for compaction ranges from ~50% for a thin sedimentary section, which would have a high average porosity, to ~20% for thick sedimentary sections, where the base of the section is already fully compacted.

The Makran subduction zone provides an upper limit for accretionary fluxes at subduction zones. There, the flux could be as high as 210 km^3/my per kilometer of subduction zone (equal to 7 km sedimentary section × 0.8 compaction factor × 37 km/my convergence velocity). It is more common to consider the

[1]Yale University, New Haven, CT.

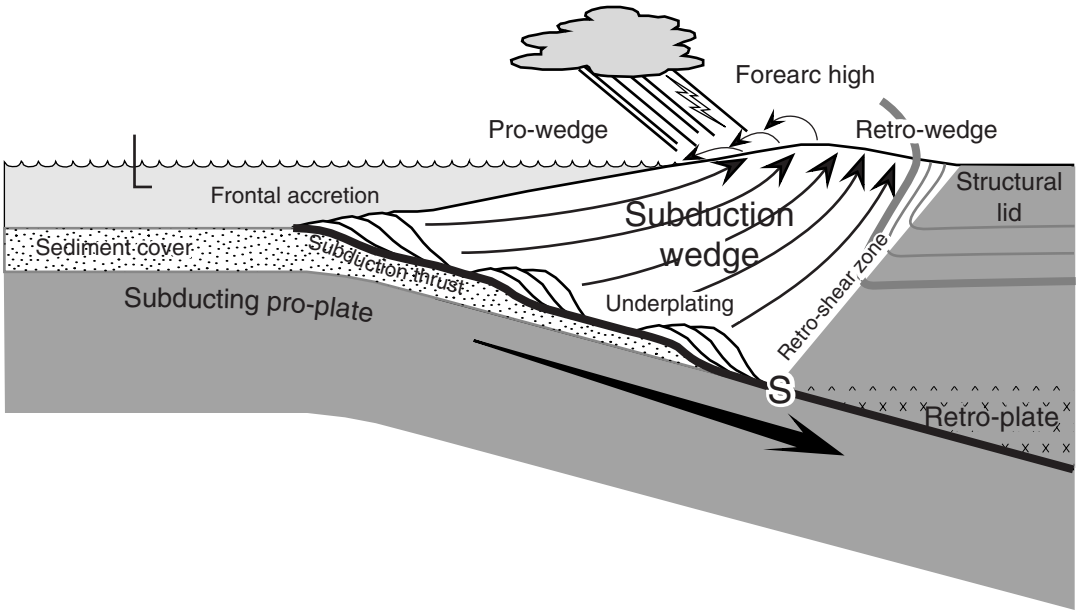

FIGURE 22.2.1 Schematic cross section of a subduction wedge. "S" refers to the S point, the subduction point, where the pro-plate is subducted beneath the retro-plate.

accretionary flux from a cross-sectional view. Thus, the flux is given as km^2/my, which represents the cross-sectional area of material added to the upper plate per unit time.

22.2.3 Wedges, Taper, and Stability

The accreted material tends to accumulate in front of and beneath the leading edge of the overriding plate, forming a wedge-shaped body that grows with time (Figure 22.2.1). A useful analogy is the way that snow piles up in front of a moving plow, forming a tapered wedge that moves with the plow (representing the overriding plate). The wedge entrains snow from the roadbed, which causes the wedge to grow (see Chapter 18).

An important discovery of the 1980s was that accretionary wedges tend to maintain a self-similar form as they grow. This behavior is expected for a wedge made of frictional materials, in that the wedge taper must be blunt enough to overcome the frictional resistance to slip on the subduction thrust that underlies the wedge. A wedge that is able to slip along its base is called a stable wedge, in that the wedge does not deform or change shape as it rides above the subduction thrust. The taper geometry of the wedge introduces an important feedback. Frontal accretion tends to drive the wedge into a substable taper, where the wedge taper is now too slender to overcome friction on the subduction thrust. The wedge becomes locked to the subducting plate, and thus must deform internally to account for the convergence velocity. The resulting horizontal shortening allows the wedge to return to its stable taper, at which point horizontal shortening stops because the wedge is now free to slip on it base. Thus, the accretionary flux into the front of the wedge controls deformation within the wedge.

Erosion will cause similar feedback, as it tends to reduce wedge taper, which causes horizontal shortening and a return to a stable taper. Erosion has a strong influence on the evolution of subaerial convergent wedges, such as the Himalaya or Alps, but subduction wedges are commonly submerged below sea level where erosion is not as active. Nonetheless, erosion can be locally important when a subduction wedge becomes emergent, which is common during the later evolution of wedges at continental subduction zones (e.g., Figure 22.2.1). Erosion acts to drive deformation and also serves to limit the growth of the wedge. This is illustrated by the examples that follow, with particular emphasis on the Cascadia margin of western North America.

22.2.4 Double-Sided Wedges

An important development in wedge theory occurred during the early 1990s, with the recognition that most convergent orogens consist of two wedges, arranged back-to-back. This idea was first proposed for collisional orogens, like the Alps, but it was also recognized as applicable for wedges that form at subduction zones.

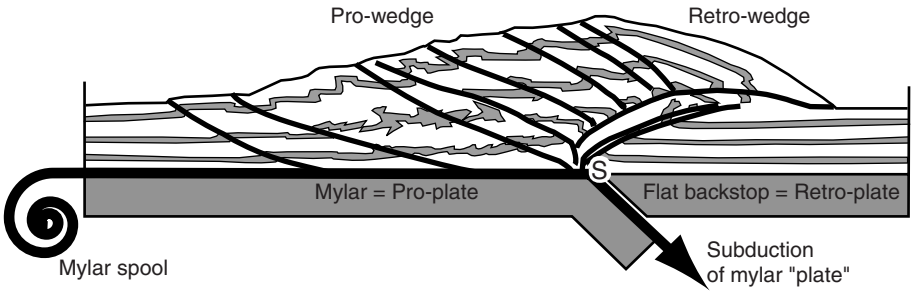

FIGURE 22.2.2 Sketch of sandbox experiment producing a double-sided wedge.

The basic problem with the snowplow analogy was that it was hard to identify where the strong plow-blade, or backstop as it is commonly called, was located within the overriding plate. Many authors used relative strength to define backstops within the crust. However, in many cases, the backstop region could be shown to be deforming along with the accreted material in front of it. This contradicted the basic idea of a backstop, which is supposed to be a rigid part of the overriding plate.

The solution to the backstop problem was inspired by sandbox experiments (Figure 22.2.2) in which a mylar sheet serves as the subducting plate and a "fixed" flat-lying plate serves as the overriding plate. This arrangement of "plates" was covered with continuous layers of sand, representing the deformable crust above the plates. A motor was then used to draw the mylar downward through a slot in the base of the sandbox, thus simulating the motion of the subducting plate. This subduction caused the overlying sand layer to deform into a double-sided wedge centered over the subduction point, or S point. The overriding plate served as a backstop, but in this case the backstop was flat-lying. Notably, there is no visible backstop at the surface. Instead, the backstop is a deep-seated structural element, with a flat-lying geometry that is hidden from view.

In a geodynamic perspective, deformation within a convergent wedge is driven by the motion of a subducting pro-plate and an overriding retro-plate. These two plates are rigid, and correspond to relatively strong lithospheric mantle, whereas the overlying crust is deformable, and thus must accommodate the velocity discontinuity at the S point. In simple terms, the model postulates that convergent wedges overlie a deep-seated mantle subduction zone. It is the cold strong mantle in the plates that controls their plate-like behavior. The crust is draped over the zone of mantle subduction, and thus deforms in a more distributed matter to accommodate subduction.

Wedges associated with subduction zones are called **accretionary wedges,** but the term has led to the thinking that the size of an actively deforming wedge is defined by the volume of accreted sediment. The concept of a double-sided wedge provides a different view, in that the active wedge involves both accreted sediments and upper-plate rocks. This result stems from the fact that the width of the wedge is determined by the motion of the underlying mantle plates, and not by any specific distribution of strength in the crust. Using terms like **subduction wedge** or **convergent wedge** when describing double-sided wedges helps to distinguish this model from that of a small wedge of accreted sediment bounded by a strong crustal backstop.

22.2.5 Subduction Polarity and Pro-Side Accretion

The term facing is used to describe the polarity of subduction. For instance, a west-facing subduction zone indicates that the overriding plate is moving westward relative to the subducting plate. This asymmetry can be ignored when measuring convergence velocities across a subduction zone, but it does have an important influence on how the wedge grows with time. Consider the situation where the pro-plate is subducted, while the retro-plate remains largely unconsumed. This asymmetry means that most of the accretionary flux is carried into the pro-side of the convergent wedge. When accretion occurs on the retro-side as well, it is always at a much slower rate than on the pro-side.

The dominance of pro-side accretion creates a strong tendency for all material in the wedge to move horizontally from the pro-side of the wedge to the retro-side. This situation is further influenced by the pattern of surficial erosion across the wedge. Consider accretion on the pro-side and strong erosion on the retro-side. This pattern of accretion and erosion will produce the greatest horizontal velocities within the wedge. An example of this situation is the Southern Alps of New Zealand, a beautiful active mountain range formed by oblique subduction of the Pacific Plate beneath the Australian Plate. The retro-wedge

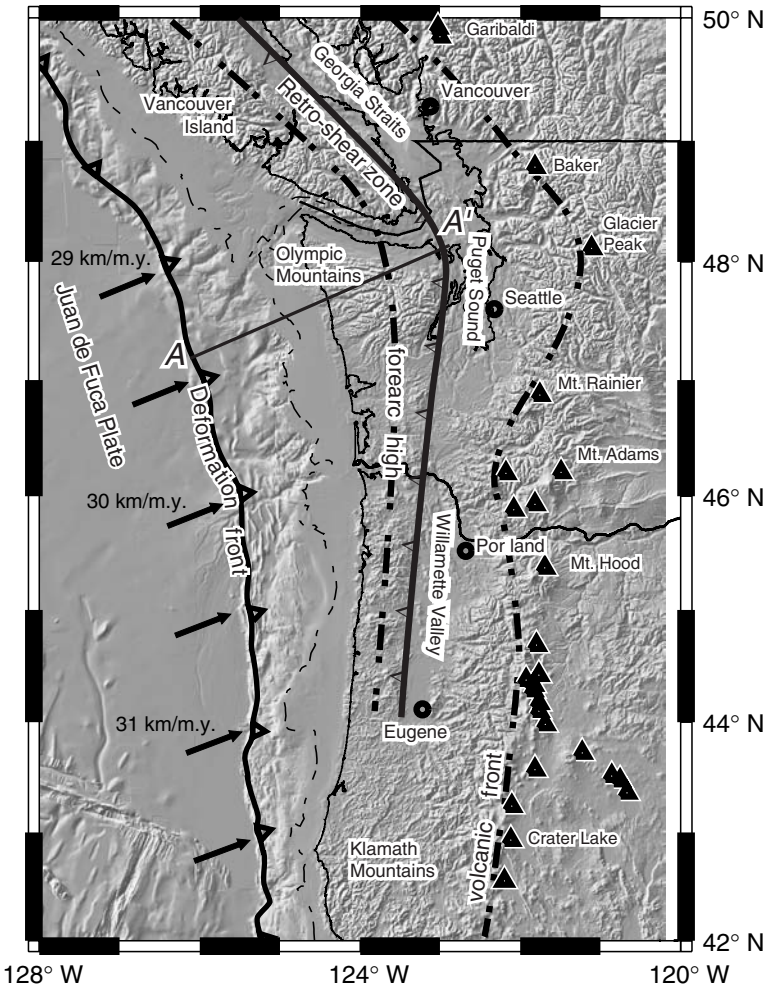

FIGURE 22.2.3 Modern tectonic setting of the Cascadia margin, emphasizing the plate boundary, volcanic arc, and physiography of the modern margin. *A-A′* shows the location of the cross section in Figure 22.2.4. Velocity vectors show the modern velocity of the Juan de Fuca Plate relative to a fixed overriding plate. Recent geodetic work has shown that the Cascade arc and forearc move as a separate plate relative to North America, due in part to deformation across the Basin and Range Province, which lies behind the southern half of the Cascade arc. The velocities shown here at the subduction zone account for this additional plate.

lies on the west side of the South Island, and is subjected to big storms coming from the Tasman Sea. Average precipitation there is more than 7 m per year, whereas the pro-wedge, located on the drier east side of the range, has an average precipitation of ~1 m per year. As a result, erosion associated with those Tasman Sea storms tends to move material from the pro-side to the retro-side of the wedge, over a horizontal distance of ~90 km.

At this point it is useful to distinguish two important geologic features within the wedge system: the structural lid and the accretionary complex. The structural lid refers to the tapered leading edge of the overriding plate, which tends to get involved in wedge deformation. The accretionary complex refers to those materials that were accreted into the wedge. The important distinction is that the structural lid originated as part of the retro-plate, whereas most, if not all, of the accretionary complex is derived by accretion from the pro-plate. From the examples that follow, we will see that, as the accretionary complex grows, the structural lid tends to get shouldered aside to the rear of the wedge. A common result is that the structural lid is only preserved within a large backfold within the retro-wedge.

22.2.6 The Cascadia Subduction Zone

The Cascadia subduction zone has a length of 1300 km and is located along the continental margin west of northern California, Oregon, Washington, and Vancouver Island (Figures 22.2.3 and 22.2.4a). In this area, the offshore Juan de Fuca Plate is actively subducting beneath an overriding North American Plate at rates of ~30 km/m.y. (arrows in Figure 22.2.3; see caption for details on estimation of convergence velocities). The direction of convergence is approximately orthogonal to the subduction zone. The surface trace of the subduction thrust is entirely submarine (deformation front in Figures 22.2.3 and 22.2.4a), lying at ~2500 m below sea level. Most of the plate convergence is accommodated by slip on the subduction thrust, but there is also a subordinate amount of shortening in the overriding subduction wedge. Slip on the subduction thrust is thought to occur episodically during great thrust

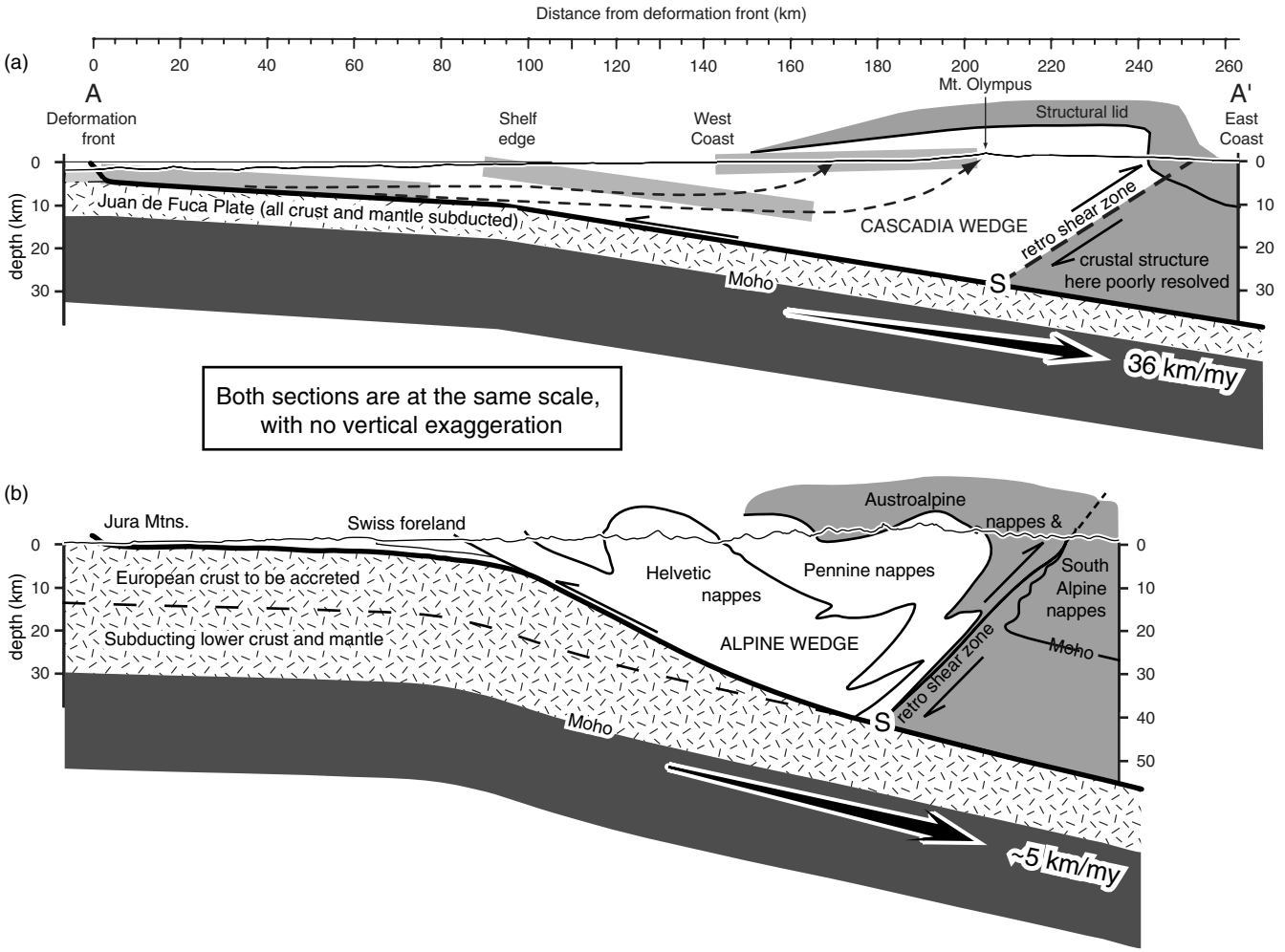

FIGURE 22.2.4 Comparison in cross section of the structure of the Cascadia margin across northwest Washington State and the structure of the European Alps across central Switzerland. The gray bands in the Cascadia section illustrate the displacement history of sediments presently exposed in the western Olympics, which were accreted at the front of the wedge at ~22 Ma and then moved rearward through the wedge, reaching the west side of the Olympics in the present.

earthquakes, with recurrence times of ~500 years. The last subduction-zone earthquake occurred on AD January 26, 1700. The Juan de Fuca Plate is covered by ~2500 m of sediment. Geophysical and geochemical evidence indicates that all of the incoming sedimentary section is accreted into the Cascadia wedge, whereas the underlying crust and mantle are fully subducted. These observations allow an estimate of the present accretionary flux of ~52 km^2/my.

The subduction zone parallels the Cascade volcanic arc, which includes active volcanoes such as Mt. Rainer. Studies at modern subduction zones indicate that the subducting slab has to reach a depth of ~100 km for melting to start in the overlying mantle. Thus, the Cascade volcanic front can be viewed as an approximate indicator of the 100-km depth contour of the downgoing slab. With this in mind, note that the distance between the subduction zone and the arc is largest across the Olympic sector of the Cascadia margin. The reason is that the dip of the subducting slab varies along the subduction zone and that the shallowest dip is found beneath the Olympic Mountains. We return to this point subsequently because the shallower dip of the slab beneath the Olympics has had a strong influence on the evolution of the Cascadia wedge in that area.

The forearc, which is the region between the arc and the subduction zone, is marked by a low and a high, both of which parallel the general trend of the subduction zone. The forearc low includes the Georgia Straits adjacent to Vancouver Island, Puget Sound of western Washington State, and the Willamette Valley of western Oregon. The forearc high corresponds to the Insular

Range, which defines Vancouver Island, and the Coast Range of western Washington and western Oregon.

The forearc high represents the crest of the Cascadia subduction wedge, with a pro-wedge to the west and a smaller retro-wedge to the east. The retro-wedge shear zone, shown in Figures 22.2.3 and 22.2.4a, marks the eastern limit of permanent deformation and uplift associated with the subduction wedge. The structure exposed there is not a fault zone, but rather a large eastward vergent "backfold," which is actively accommodating slow, top-to-east shear between the retro-wedge and the forearc low. The forearc low is commonly viewed as a basin, but there has been little subsidence or sediment accumulated in this low over the last 10 to 15 my. Instead, the low is defined by the volcanic arc to the east and the actively growing forearc high to the west.

Geologic evidence indicates that the Olympic Mountains mark the first part of the Cascadia forearc high to emerge above sea level, at ~15 Ma. The forearc high apparently grew more slowly elsewhere along the margin. In fact, Vancouver Island and the southern part of the Coast Ranges may have emerged above sea level only within the last 5 to 10 my. The early emergence of the forearc high in the Olympics may reflect a slab that is shallower there. To understand this situation, consider that the growth of a subduction wedge is controlled by the accretionary flux into the wedge and erosion of the forearc high. Erosion cannot start until the forearc high becomes subaerially exposed, but once the wedge does become emergent, erosion will act to slow the growth of the wedge, until it reaches a flux steady state, when the erosional outflux becomes equal to the accretionary influx.

It was already noted that the subducting slab has a shallower dip beneath the Olympics relative to adjacent parts of the subduction zone. This archlike form of the subducting slab is apparent when one considers the depth of the slab beneath the forearc high, which is equal to ~40 km beneath Vancouver Island, ~30 km beneath the Olympics, and ~40 km beneath southwest Washington State. This variation in slab depth cannot be attributed to variations in topography, because the mean elevation of the forearc high varies by only a small amount, between ~500 to 1000 m along its length. Thus, this configuration may be a fundamental feature of the subduction geometry of the slab.

The important point here is that the wedge beneath the Olympics is much smaller than elsewhere along the margin. Thus, given a similar accretionary flux, less time was needed for the forearc high to become emergent in the Olympics relative to other parts of the subduction wedge.

Erosion of the Forearc High

The effect that erosion has on deformation and growth of the wedge was noted earlier. Several methods were used to measure the long-term erosional flux coming out of the Olympics part of the forearc high. One method is **apatite fission-track dating,** which dates when a sample cooled below the apatite fission-track closure temperature (~110°C). A thermal model is used to convert the closure temperature to a depth, with results that typically lie in the range of 3–5 km. Dividing depth by cooling age gives the average erosion rate for the time interval represented by the cooling age.

Another method involves measuring the **incision rate** of rivers, which is the rate at which a river cuts downward into bedrock. The rate of channel incision can be determined from old river deposits preserved on the hillslopes adjacent to the river. These deposits commonly overlie old remnants of the river channel where it was running on bedrock. The height of these paleochannel remnants above the modern channel divided by the age of the paleochannel gives the incision rate of the river.

In the Olympics, paleochannel remnants formed at ~65 ka and 140 ka produced 60 incision rates along the Clearwater River, which drains the west side of the forearc high. Apatite fission-track ages provide another 43 estimates of erosion rates, with average cooling ages of ~7 my. These data are shown in Figure 22.2.5, where they have been projected into the section line *A*-*A′* (Figure 22.2.4) across the subaerially exposed part of the forearc high. Particularly interesting is the similarity between incision rates and fission-track-based erosion rates, despite the fact that they represent local versus regional processes and different intervals of time as well; that is, 100 ky versus 7 my. Recently (U-Th)/He apatite dating found younger cooling ages of ~2 my, which reflect the lower closure temperature (~65°C) for this thermochronometer. The erosion rates indicated by these ages (not shown) also match closely the rates shown in Figure 22.2.5. The conclusion is that, when viewed on timescales longer than ~50 ky, the pattern and rates of erosion across the forearc high appear to have been fairly steady.

Let's compare these rates with the accretionary flux that we estimated previously. We use the data in Fig-ure 22.2.5 to estimate the integrated erosional flux from the forearc high. The curve provides a smoothed version of the data and is used to integrate the flux. This gives an erosional flux of 51 km^2/my. Our thermal-kinematic modeling gives a more precise estimate of 57 km^2/my. Both estimates are similar to the accretionary flux, 52 km^2/my, estimated

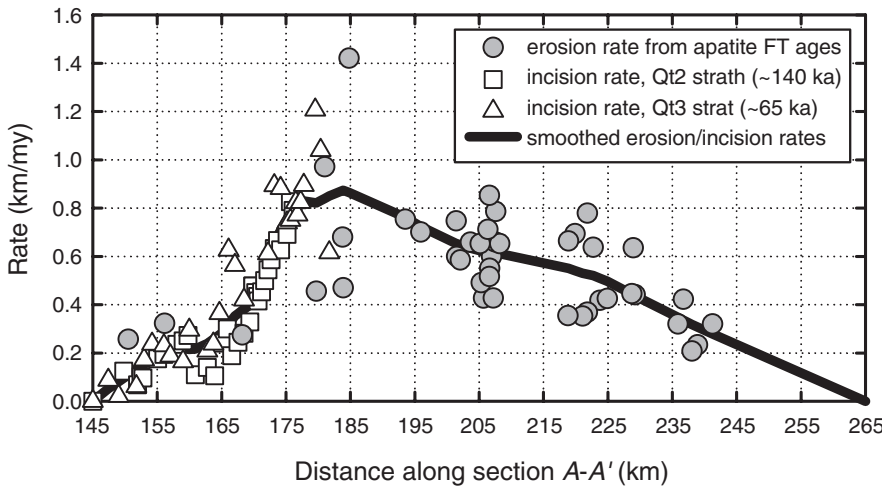

FIGURE 22.2.5 Fluvial incision rates and long-term erosion rates determined from apatite fission-track ages. The fluvial incision rates represent downcutting of the Clearwater River over a timeframe of ~100 ka, whereas the fission-track ages indicate erosion rates over a time frame of ~7 my. The similarity in rates suggests that the pattern and rates of erosion have been steady across this part of the forearc high. The black curve represents a smoothed version of the erosion rate distribution across the high. Integration of this curve indicates that the long-term erosional flux from the forearc high is ~51 km^2/my.

previously, showing that there is a close balance between accretionary flux into the wedge and the erosional flux out of the wedge. Thus, the wedge cannot get any larger with time. Even so, the material within the wedge will still continue to move and deform, given that an eroding wedge must thicken to maintain a stable taper.

(U-Th)/He apatite dating in other parts of the Cascadia forearc arc high shows that everywhere else the forearc high has been only slightly eroded, by less than 3 km. Estimates of erosion rates suggest that these regions have only recently become emergent and have yet to reach the steady-state configuration observed in the Olympic Mountains. It would be interesting to predict how much time is needed for a growing subduction wedge to reach a steady-state configuration. To do so requires a better understanding of how local-scale erosional processes scale up in time and space to account for the large-scale evolution of orogenic topography. This is an area of active research, with much promise for new discoveries.

DEFORMATION AND EROSION OF THE STRUCTURAL LID

How have accretion and erosion influenced the longer-term evolution of the Cascadia wedge? Prior to initiation at ~35 Ma, the continental margin included a large oceanic terrane, Eocene in age, called the Crescent terrane. This terrane was already part of the outboard edge of the North American Plate, having been accreted to North America prior to 35 Ma. Thus, when the Cascadia subduction zone was initiated, the Crescent terrane became the structural lid for the subduction zone (Figure 22.2.4a).

Uplift and erosion in the Olympics provide a good sectional view of the Crescent terrane (Figures 22.2.4a and 22.2.6). It consists of relatively coherent Eocene oceanic crust, mostly pillowed flows of basalt, which are typical of submarine volcanism. Exposures along the north side of the Olympic Mountains show the tapered form of the structural lid (Figure 22.2.6). Across the 120-km width of the forearc high, the basaltic sequence changes from 4 km thickness in the west to more than 15 km in the east. This tapered geometry marks the original eastward dip of the Cascadia subduction zone when it was first formed. At that time, the lower part of the Crescent terrane was apparently subducted, leaving behind the tapered lid, which then became the highest structural unit within the Cascadia wedge.

In the Olympic Mountains, the structural lid is underlain by an accretionary complex, called the Olympic subduction complex. In cross section, this unit is 240 km across and extends to a depth of at least 30 km, giving it a cross-sectional area of 3600 km^2. Seismic studies indicate that this accretionary complex is made up entirely of sedimentary rocks; there is no evidence of basaltic crust or mantle from the subducting plate. Seismic reflection profiles across southern Vancouver Island indicate that the Crescent terrane there is also underlain by a large volume of low-velocity layered rocks, similar to the Olympic subduction complex. Given the present accretionary flux, it would take ~70 my to grow an accretionary complex this size, which is much longer than the 35 my age of the Cascadia subduction zone. Evidence in the Olympics indicates that the more internal parts of the accretionary complex are made up of sedimentary sequences that probably predated the subduction zone. This makes sense, given that the newly formed subduction zone cut across a preexisting continental margin. Thus the sedimentary units that flanked that margin were probably the first to be accreted.

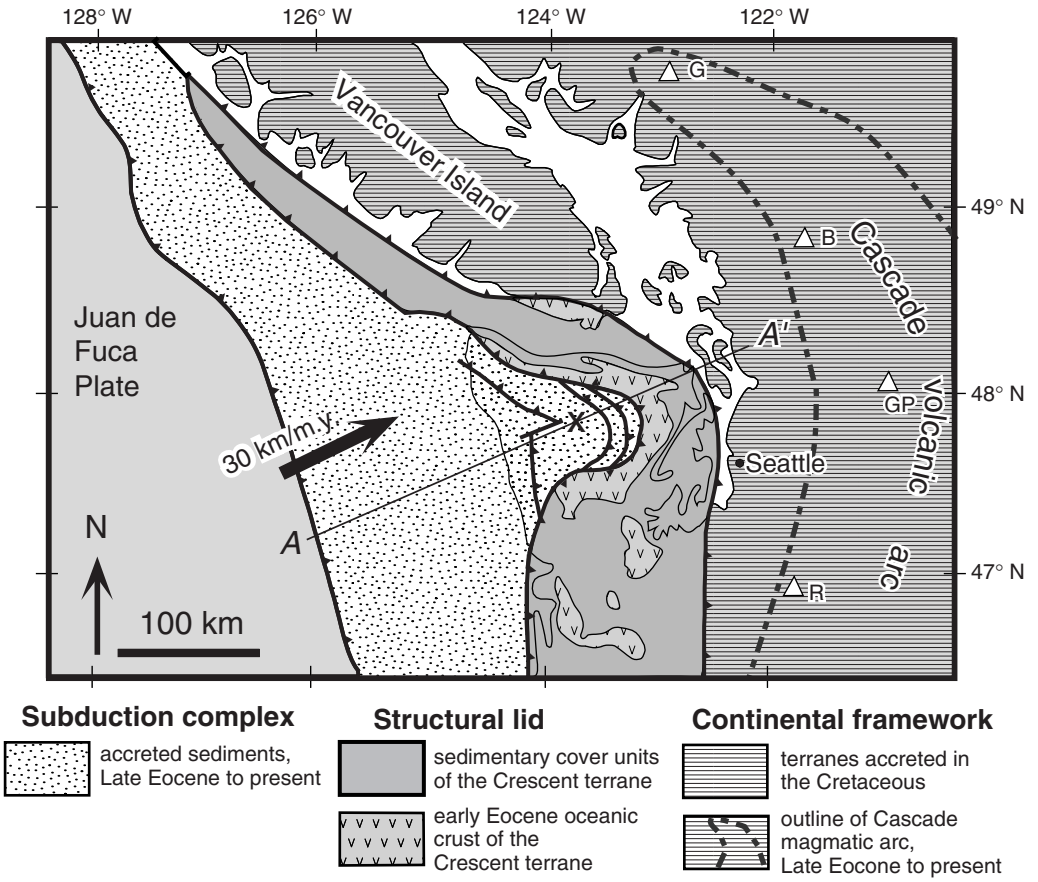

FIGURE 22.2.6 Geology of the Cascadia margin, emphasizing the present configuration of the structural lid. "X" marks Mount Olympus, which is the highest summit (2,428 m) in the Washington-Oregon Coast Range. *A-A′* indicates the location of the cross section shown in Figure 22.2.3. Major volcanoes of the Cascadia arc are: G = Mt. Garibaldi, B = Mt. Rainier, GP = Glacier Peak, R = Mt. Rainier.

In the Olympics, the structural lid has slowly been driven into the back of the wedge system as the accretionary part of the wedge has grown in size. Initially, the lid was uplifted into a broad arch, as observed in the Oregon Coast Range. When this arch became emergent, it started to erode, which allowed the lid to rise faster. As the lid was removed, the accretionary complex moved rearward to take its place. This motion was required for the wedge to maintain a stable taper, as discussed earlier.

The end result is that the lid was driven rearward, creating a large fold. This fold is actually the manifestation of a broad, west-dipping retro-shear zone, which accommodates the top-east motion of material within the retro-wedge. This structure is quite impressive in the Olympics. One can drive into the mountain range from the east, where the Crescent terrane is still flat-lying and undeformed. Moving west across the range front, one notices that the Crescent starts to dip to the east, which marks the fact that we have crossed into the upper limb of the back fold. The dip continues to increase until the section becomes vertical, and locally overturned. This increase in limb dip is also accompanied by a dramatic topographic gradient, which marks the east-dipping surface of the retro-wedge. Within 20 km, the topography rises from sea level to over 2300 m.

The Olympics represents the most evolved part of the Cascadia forearc high, as indicated by uplift, erosion, and backfolding of the structural lid. Elsewhere along the Cascadia margin, the structural lid still covers the forearc high. This difference in evolution of the margin accounts for the large reentrant in the Crescent terrane centered on the Olympic Mountains. Other parts of the forearc high continue to grow, but that growth has only resulted so far in a broad arching of the structural lid. The prediction is that with further deformation and erosion, those other parts of the forearc high will evolve towards the structural configuration observed in the Olympics.

22.2.7 Comparison between the Cascadia and Alpine Wedges

The cross sections in Figure 22.2.4 offer a comparison between the Cascadia wedge and Europe's Alpine wedge (see Subchapter 21.1). The Swiss Alps are different in that they formed by collision of two continental plates, starting ~50 Ma. Convergence there has slowed down, and perhaps stopped within the last 5 my The average Alpine convergence rate is ~5 km/my, which is slower than the Cascadia convergence by a factor of six. However, in the European Alps, the pro-thrust cuts much more deeply into the pro-plate, resulting in accretion of the upper 15 km of crust from the pro-plate (Figure 22.2.4b). The associated accretionary flux for the Alps is therefore estimated ~75 km^2/my, which is slightly larger than for the Cascadia wedge. Nevertheless, the Alpine wedge is smaller than the Cascadia wedge, but because the Alpine wedge is entirely subaerial, erosion was able to more effectively limit the size of the wedge.

This comparison highlights the similarities in backfolding of the structural lid. In the European Alps, the structural lid is made up of crustal rocks belonging to the Southern Alpine and Austroalpine nappes (Section 21.1). These nappes are thrust sheets associated with the tapered leading edge of the overriding continental plate, which is called the Adriatic Plate. As in the Olympics, the tapered geometry of the structural lid reflects the cut made through the upper plate by the subduction thrust when subduction was initiated. Accretion from the pro-side is responsible for driving the structural lid rearward in the wedge. The Alpine geologists call this retrocharriage, meaning "to carry back." The resulting backfold underlies the southern flank of the Alps.

ADDITIONAL READING

Batt, G. E., Brandon, M. T., Farley, K. A., and Roden-Tice, M., 2001. Tectonic synthesis of the Olympic Mountains segment of the Cascadia wedge, using two-dimensional thermal and kinematic modeling of thermochronological ages. *Journal of Geophysical Research,* 106, 26731–26746.

Beaumont, C., Ellis, S., and Pfiffner, A., 1999. Dynamics of sediment subduction-accretion at convergent margins: short-term modes, long-term deformation, and tectonic implications. *Journal of Geophysical Research,* 104, 17573–17602.

Brandon, M. T., Roden-Tice, M. K., and Garver, J. I., 1998. Late Cenozoic exhumation of the Cascadia accretionary wedge in the Olympic Mountains, Northwest Washington State. *Geological Society of America Bulletin,* 110, 985–1009.

Clowes, R. M., Brandon, M. T., Green, A. G., Yorath, C. J., Sutherland Brown, A., Kanasewich, E. R., and Spencer, C., 1987. LITHOPROBE-southern Vancouver Island: Cenozoic subduction complex imaged by deep seismic reflections. *Canadian Journal of Earth Sciences,* 24, 31–51.

Dahlen, F. A., 1990. Critical taper model of fold-and-thrust belts and accretionary wedges. *Annual Review of Earth and Planetary Sciences,* 18, 55–99.

Escher, A., and Beaumont, C., 1997. Formation, burial, and exhumation of basement nappes at crustal scale; a geometric model based on the western Swiss-Italian Alps. *Journal of Structural Geology,* 19, 955–974.

Jarrard, R. D., 1986. Relations among subduction parameters. *Reviews of Geophysics,* 24, 217–284.

Malavieille, J., 1984. Modelisation experimentale des chevauchements imbriques; application aux chaines de montagnes. *Bulletin de la Societé Géologique de France,* 26, 129–138.

Pazzaglia, F. J., and Brandon, M. T., 2001. A fluvial record of long-term steady-state uplift and erosion across the Cascadia forearc high, western Washington State. *American Journal of Science,* 301, 385–431.

Stewart, R. J., and Brandon, M. T., 2003. Detrital zircon fission-track ages for the "Hoh Formation": implications for late Cenozoic evolution of the Cascadia subduction wedge. *Geological Society of American Bulletin,* 115, in press.

von Huene, R., and Scholl, D. W., 1991. Observations at convergent margins concerning sediment subduction, subduction erosion, and the growth of continental crust. *Reviews of Geophysics,* 29, 279–316.

Willett, S. D., and Brandon, M. T., 2002. On steady states in mountain belts. *Geology,* 30, 175–178.

Willett, S., Beaumont, C., and Fullsack, P., 1993. Mechanical models for the tectonics of doubly vergent compressional orogens. *Geology,* 21, 371–374.